ELSEVIER

Biochimica et Biophysica Acta 1515 (2001) 159–166

BIOCHIMICA ET BIOPHYSICA ACTA
BBA

www.bba-direct.com

Escherichia coli OmpA retains a folded structure in the presence of sodium dodecyl sulfate due to a high kinetic barrier to unfolding

Satoshi Ohnishi *, Keiichi Kameyama [1]

Institute for Protein Research, Osaka University, Yamadaoka 3-2, Osaka, Suita, 565-0871, Japan

Received 9 May 2001; received in revised form 28 August 2001; accepted 30 August 2001

Abstract

Escherichia coli OmpA can be solubilized by sodium dodecyl sulfate (SDS) in its folded structure, and it unfolds upon heating. Although the heat-denatured OmpA remains unfolded after lowering the temperature, the addition of a non-ionic surfactant, octyl glucoside results in refolding of unfolded OmpA. In the present study, we investigated the refolding kinetics of OmpA in a mixed surfactant system of SDS and octyl glucoside using far- and near-UV circular dichroism and fluorescence spectroscopies. We found four kinetic phases in the refolding reaction, which logarithmically depended on the weight fraction of octyl glucoside. We also examined the unfolding kinetics of OmpA upon heating in the presence of SDS by temperature jump experiments. A comparison of the rate constants for the refolding and the unfolding reactions in SDS-only solution at 30°C revealed that the folded form of OmpA in SDS solution is less stable than the unfolding form, and that the unfolding is virtually unobservable near room temperature due to a high kinetic barrier.

Keywords: Folding kinetics; Membrane protein; OmpA; Protein folding; Stability

1. Introduction

Membrane proteins fold into their native structure only under amphiphilic conditions, and the requirement of amphiphiles presents an experimental limitation in biophysical and structural research. In the last decade, significant experimental data for conformational changes have accumulated for several membrane proteins such as bacteriorhodopsin [1–5], the major photosynthetic antenna complex of green plants [6], diacylglycerol kinase [7], OmpF porin [8,9], and OmpA [10–15]. Most of those experiments have been performed in a mixture of lipid and denaturant, that of lipid and surfactant or that of different surfactants. Formation of the tertiary structure of a membrane protein under such amphiphilic conditions should be driven by interactions between the polypeptide and the external amphiphilic media. A mixed system of a surfactant with strong denaturing

Abbreviations: CD, circular dichroism; ΔG, free energy of unfolding; $\Delta G^{\ddagger}_{SDS}$, free energy of activation upon denaturation in the presence of SDS; h-OmpA, heat-modified OmpA; OG, *n*-octyl β-D-glucoside; PAGE, polyacrylamide gel electrophoresis; SDS, sodium dodecyl sulfate; X_{OG}, weight fraction of OG in the mixed surfactant system of SDS and OG

* Corresponding author. Present address: Department of Biochemistry and Biophysics, University of Rochester Medical Center, 601 Elmwood Avenue Box 712 Rochester, NY 14642, USA. Fax: 716-275-6007.

E-mail address: satoshi_ohnishi@urmc.rochester.edu (S. Ohnishi).

[1] Present address: Faculty of Engineering, Gifu University, Yanagido 1-1, Gifu, 501-1193, Japan.

0005-2736/01/$ – see front matter
PII: S0005-2736(01)00410-2

ability and that with little denaturing ability can be used to systematically control the denaturing activities, making it possible to quantitatively assess the folding properties of a membrane protein.

We previously examined the refolding property of a membrane protein, *Escherichia coli* OmpA, in the mixed surfactant system of sodium dodecyl sulfate (SDS) and octyl glucoside (OG) [16]. OmpA is a 35 kDa membrane protein consisting of a transmembrane N-terminal domain and a periplasmic C-terminal domain [17,18]. The 19 kDa N-terminal domain is an eight stranded β-barrel (Fig. 1) [19,20], while the structure of the C-terminal domain is unknown. OmpA can be solubilized in a monomeric, folded form in the presence of SDS at room temperature. As we will show below, the folded form of OmpA in SDS solution showed a far-UV circular dichroism (CD) spectrum typical of a β-sheet, which was quite similar to that observed in lipid vesicles [11]. On the other hand, the structure of the C-terminal domain is unknown, and the protein structure in surfactant micelles may be different from that in the outer membrane of *E. coli* due to the difference in distribution of hydrophobic and hydrophilic atmosphere between surfactant micelles and the lipid bilayer. Therefore, we do not use the term 'native form' in the present study to describe the folded form of OmpA in surfactant solutions. The folded form of OmpA in the presence of SDS denatures upon heating, which is commonly described as 'heat modifiability' [21]. The heat-induced conformational change is virtually irreversible, and this heat-modified form, i.e. denatured form upon heating in the presence of SDS, remains unfolded by lowering the temperature. This heat-modified form will be referred to hereafter as h-OmpA. The addition of OG to h-OmpA results in refolding to its folded form [22]. We previously found that the refolding of h-OmpA occurs in a cooperative manner when the weight fraction of OG (X_{OG}) in the total amount of the surfactants exceeds 0.7, suggesting that a decrease in denaturing activity of SDS triggers the refolding reaction [16]. However, this denaturing activity of SDS is inconsistent with the fact that OmpA solubilized in the presence of SDS retains the folded structure. Therefore, we hypothesized that OmpA in SDS solution at room temperature could be in a metastable form with a high kinetic barrier to unfolding, and heating reduces this kinetic barrier toward the heat-modified form. In the present study, we examined the kinetics of the conformational change of OmpA in a binary surfactant system of SDS and OG. We monitored the refolding kinetics using near- and far-UV CD and fluorescence spectroscopies. This approach revealed multiple folding steps of OmpA. We also examined the unfolding kinetics of OmpA in the presence of SDS upon heating. Our results supported the hypothesis of solubilized OmpA with SDS being metastable.

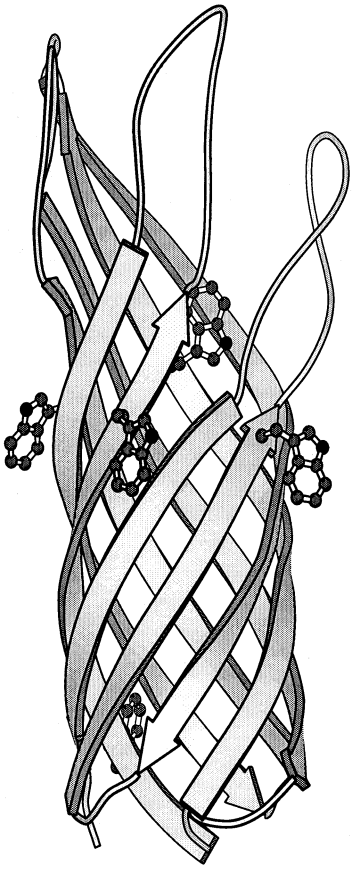

Fig. 1. Crystal structure of the transmembrane N-terminal domain (1–171) of OmpA [19,20]. Outer surface loops are shown on top, and five tryptophan residues are shown in ball-and-stick representation. The drawing was made using MOLSCRIPT [31].

2. Materials and methods

2.1. Materials

SDS was obtained from BDH (Anala R grade),

and *n*-octyl β-D-glucoside (OG) was from Dojindo Laboratories (Kumamoto, Japan). OmpA was purified from *E. coli* K-12, TNE001 strain as described previously [23]. The purified OmpA fraction was equilibrated in 50 mM sodium phosphate buffer (pH 6.9) containing 0.1% (v/v) of SDS using a size exclusion HPLC column, G3000SW$_{XL}$ (30×0.78 cm I.D., Tosoh, Tokyo, Japan). The OmpA fraction was heated in boiling water for 5 min to obtain h-OmpA.

2.2. Circular dichroism measurements

CD spectra were taken at 30°C on a J-720 spectrophotometer (Jasco, Tokyo, Japan). For far-UV (205–250 nm) CD measurements, a cuvette with 1 mm path length was used for samples with 7–12 μM of protein concentration. For near-UV (250–320 nm) CD measurements, a cuvette with 1 cm path length was used for samples with 17–22 μM of protein concentration.

2.3. Fluorescence measurements

Measurements were made on a F-4500 fluorescence spectrometer (Hitachi, Tokyo, Japan). A cuvette with 1 cm path length was used. Protein concentration was set at 1 μM. Wavelengths for excitation and emission were 296 nm and 330 nm, respectively.

2.4. Refolding experiments

The kinetic measurements by either CD or fluorescence spectroscopy were started 15 s after manually mixing a refolding buffer with h-OmpA solution. The refolding buffer contained 0.1% (v/v) SDS and a defined amount of OG in 50 mM sodium phosphate buffer (pH 6.9). The change in ellipticity was monitored at 207 nm and 289 nm, and the change in fluorescence emission intensity was monitored at 330 nm.

2.5. Temperature jump unfolding experiments

OmpA solution containing 0.1% (v/v) SDS was transferred to a cuvette that had been kept at a defined temperature, and the change in ellipticity at 207 nm was monitored. The lag time during which the temperature of the sample solution equilibrates to the defined temperature was measured by separate experiments with a blank solution.

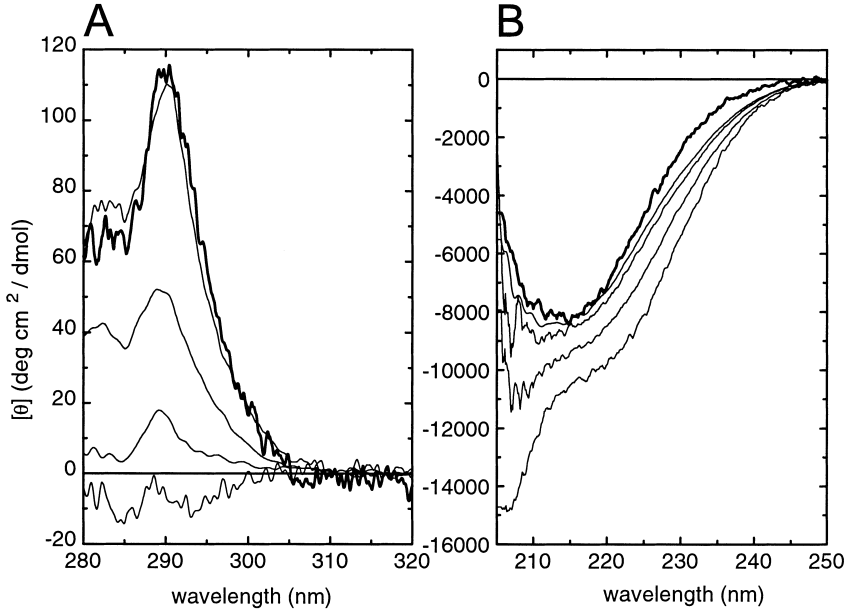

Fig. 2. CD spectra in near- (A) and far-UV (B) regions for h-OmpA in various compositions of the SDS and OG mixed system. From bottom to top, $X_{OG}=0$, 0.79, 0.81 and 0.97, respectively. The far- and near-UV CD spectra of non-heated OmpA at $X_{OG}=0$ are shown with a thick line. All the spectra were recorded after 15 h incubation at 30°C.

3. Results

3.1. Change of spectroscopic properties of OmpA observed with a change in the surfactant composition

First, we carried out an equilibrium study on the conformational change of OmpA in a mixture of SDS and OG using far- and near-UV CD spectroscopies (Fig. 2). Since OmpA has five tryptophan residues that are located only in the N-terminal domain (Fig. 1), monitoring the conformational change using these multiple probes would be appropriate to detect folding intermediates. The near-UV spectrum of h-OmpA at $X_{OG} = 0$ did not show characteristic peaks in the range from 280 nm to 320 nm, suggesting that the aromatic side chains in OmpA do not have well-defined configurations. With the addition of OG, two peaks appeared around 284 nm and 289 nm, and their ellipticities increased with an increase of the weight fraction of OG, and the spectrum at $X_{OG} = 0.97$ is almost identical to that of non-heated OmpA (Fig. 2A). Thus, OmpA in the heat-modified form refolded into the non-heated form at $X_{OG} = 0.97$ in terms of the tertiary structure of the N-terminal domain. As shown in Fig. 2B, the far-UV CD spectrum of h-OmpA at $X_{OG} = 0$ had a negative peak around 207 nm and a shoulder around 222 nm. With increasing X_{OG}, the negative peak and shoulder disappeared and the spectrum was converted to one with a minimum around 215 nm, typical of a β-sheet. At $X_{OG} = 0.97$, the far-UV CD spectrum was very similar to that of non-heated OmpA at $X_{OG} = 0$, suggesting that h-OmpA refolds to the non-heated form by the addition of OG in terms of secondary structure. The spectrum of h-OmpA at $X_{OG} = 0.97$ was almost identical to that of non-heated OmpA at $X_{OG} = 1.0$ (data not shown), and it differed from that of non-heated OmpA at $X_{OG} = 0$ in the region around 230–240 nm (Fig. 2B). The spectrum of non-heated OmpA at $X_{OG} = 0$ and that at $X_{OG} = 1.0$ were convertible by reciprocally replacing SDS and OG, and both spectra were very similar around 215 nm where β-sheet proteins show a characteristic minimum. Moreover, near-UV CD spectra of h-OmpA at $X_{OG} = 0.97$ and OmpA at $X_{OG} = 0$ were almost identical (Fig. 2A). Therefore, the difference in these spectra may not arise from a structural difference in the transmembrane domain but the periplasmic C-terminal domain.

The ellipticities of h-OmpA at 207 nm, 217 nm and 289 nm changed with the increase of X_{OG} in a cooperative manner with one transition, of which the midpoint was around $X_{OG} = 0.78$ (Fig. 3A). This is consistent with our previous results that h-OmpA refolded above $X_{OG} = 0.7$ in terms of mobility on SDS–PAGE, hydrodynamic radius and the amount of surfactant bound to the protein [23]. It should be noted that the midpoint of the transition significantly shifted to smaller X_{OG} over time (Fig. 3B), indicating that the refolding reaction had not reached an equilibrium after 15 h incubation at room temperature. The result suggests that the refolding reaction is very slow around $X_{OG} = 0.75$. As we will show below, it would take months to years for the reaction to reach an equilibrium at lower X_{OG}.

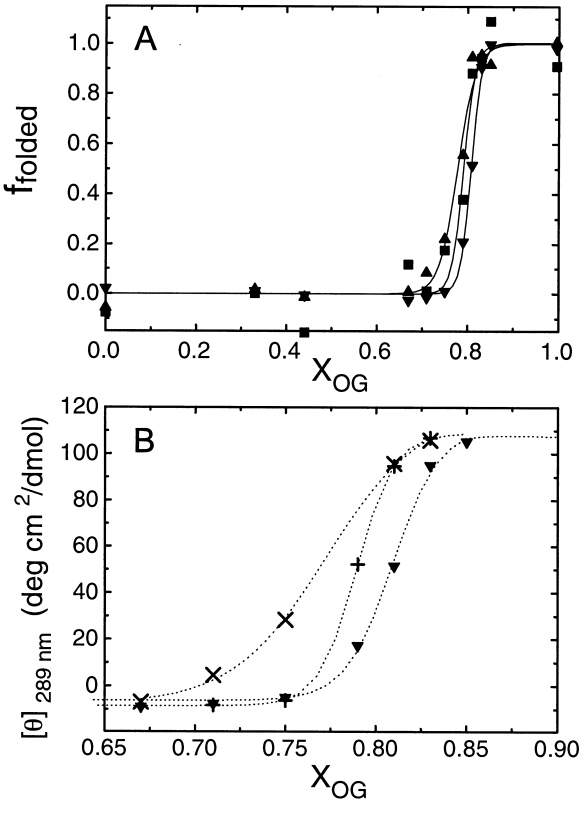

Fig. 3. (A) Fraction of folded OmpA plotted against the weight fraction of OG, obtained based on ellipticities at 207 nm (■), 217 nm (▲) and 289 nm (▼) in the spectra measured 15 h after the addition of OG. (B) Changes in the ellipticity of OmpA at 289 nm against the fraction of OG measured 15 h (▼), 4 days (+) and 14 days (×) after the addition of OG.

3.2. Refolding kinetics of OmpA from its heat-modified form

We then examined the refolding kinetics of h-OmpA initiated by the addition of OG. Fig. 4 shows typical profiles of the refolding kinetics of h-OmpA. The observed amplitudes fully accounted for those expected from equilibrium experiments, suggesting that the manual mixing technique was sufficient to follow kinetics of the refolding reaction. We did not visually detect aggregation of OmpA during this refolding reaction.

All the profiles were analyzed by fitting using an exponential function with three rate constants:

$$Y = Y_0 + A_1 \exp(-k_1 t) + A_2 \exp(-k_2 t) + A_3 \exp(-k_3 t) \quad (1)$$

Here, A_1, A_2 and A_3 are amplitudes, k_1, k_2 and k_3 are rate constants and Y_0 is the final value of the profile. Residuals of fitting with this equation scatter uniformly over the measuring time scales for all profiles (Fig. 4). In contrast, similar curve-fitting analyses using an exponential equation with one rate constant and one with two rate constants showed systematic deviations in residuals (data not shown). All rate constants thus obtained from the three spectroscopic probes showed a logarithmic dependence on the weight fraction of OG (Fig. 5). We obtained nine kinds of rate constants from these three probes, which were classified into four groups. These data suggest that the overall process of the refolding reaction can be described using four kinetic phases. Similar multi-step folding of OmpA was also observed in different experimental systems where

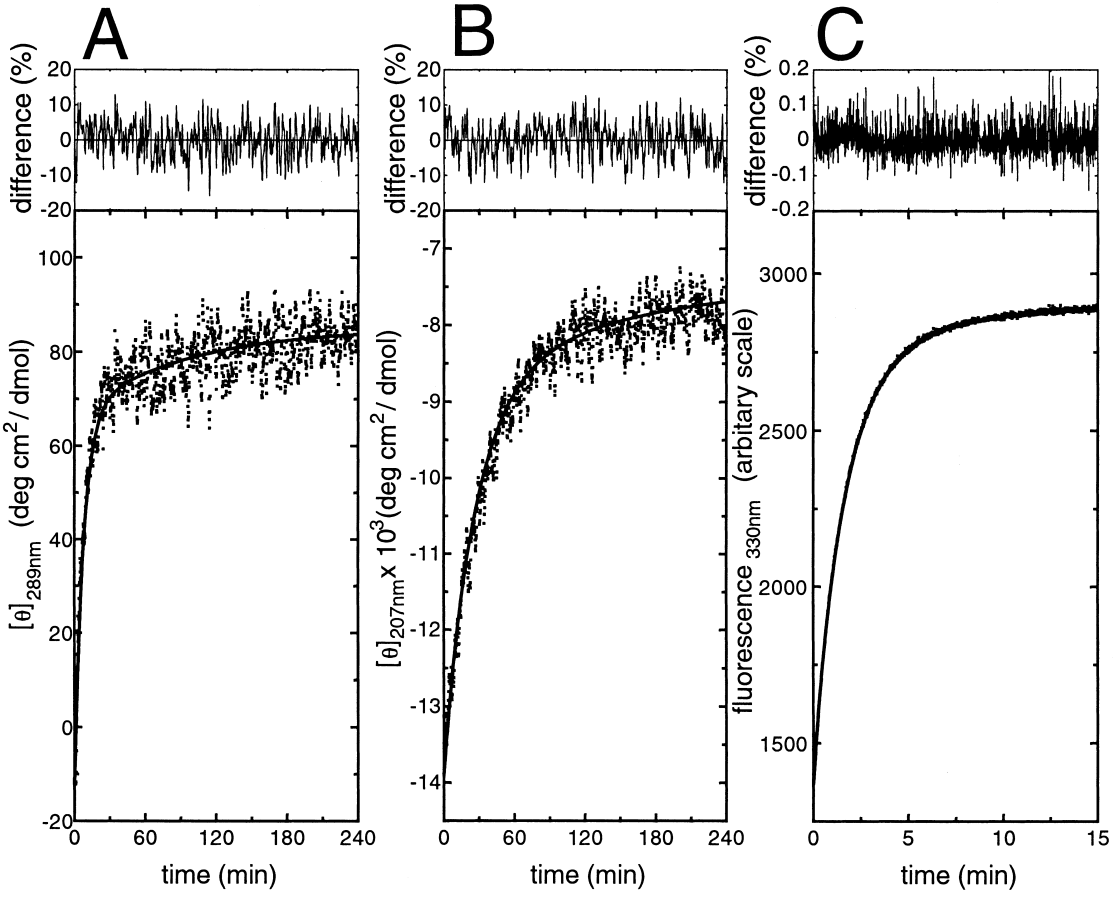

Fig. 4. Representative kinetic profiles of the refolding of h-OmpA by the addition of OG observed in ellipticity at 289 nm (A), at 207 nm (B) and fluorescence emission intensity (C). The final weight fractions of OG are 0.88 (A), 0.86 (B) and 0.88 (C). Temperature was controlled at 30°C. Upper panels show the residuals of fitting to Eq. 1 (see text). Residuals are shown as the percentages against overall change of the ellipticities or fluorescence intensity.

OmpA denatured in the presence of 8 M urea without surfactant was refolded into lipid vesicles [10–14].

3.3. Unfolding kinetics of OmpA in the presence of SDS upon heating

The unfolding kinetics of OmpA in SDS solutions monitored by the ellipticity at 207 nm in temperature jump experiments could be fitted well by a single exponential function (Fig. 6A). Accordingly, unfolding rate constants at various temperatures were determined using a single exponential function. The delay times, the times required to equilibrate the temperature of the solution, were less than 10% of the half-life of the unfolding kinetics for all the temperatures studied. The Arrhenius plots of the unfolding rate constants of OmpA gave a fairly linear correlation with the inverse of temperature (Fig. 6B). Assuming a linear correlation, the unfolding rate constant at 30°C was estimated to be 9.6×10^{-9} s^{-1}, corresponding to a half-life of 3.3 years. Although this estimate likely has large errors, our results clearly demonstrated that the denaturation of OmpA by SDS is virtually unobservable near room temperature.

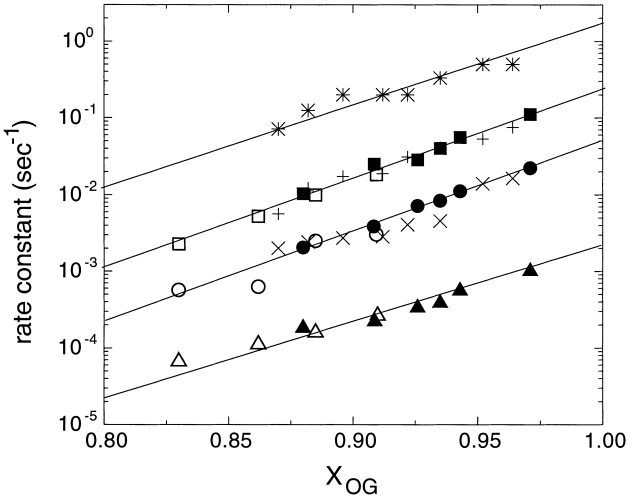

Fig. 5. The refolding rate constants of h-OmpA plotted versus the fraction of OG. The largest rate constants (k_1), the second ones (k_2) and the smallest ones (k_3) obtained from the analyses for the fluorescence kinetic profiles are symbolized as *, + and ×, respectively. Those for the near-UV CD profiles are shown as □, ○ and △, respectively, and those for the far-UV CD profiles are shown as ■, ● and ▲, respectively. The lines are drawn assuming a logarithmic correlation of the rate constants with X_{OG}.

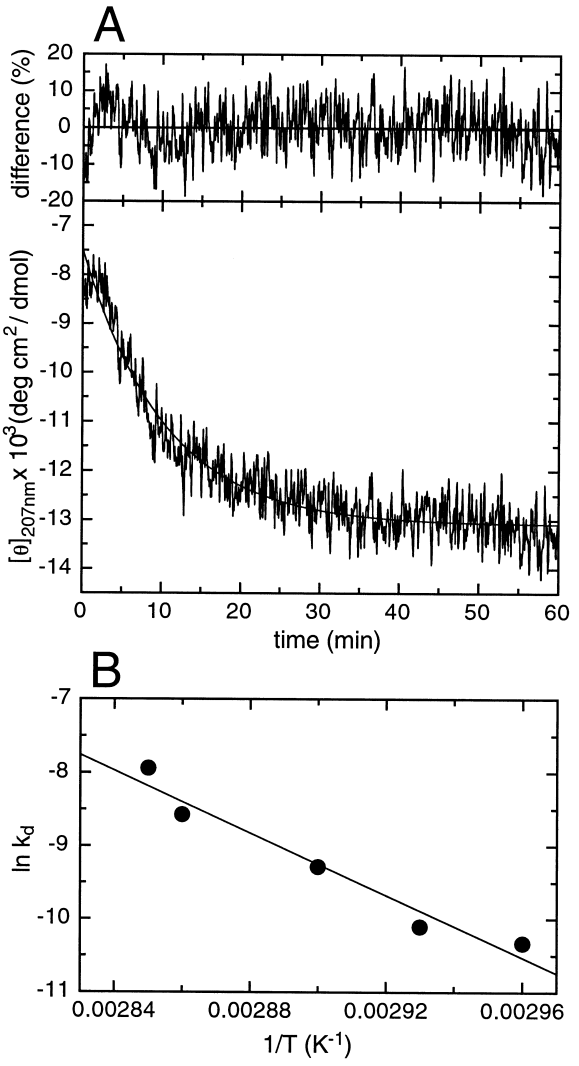

Fig. 6. (A) A representative profile of the unfolding kinetics of OmpA at $X_{OG}=0$ initiated by a temperature jump to 78.2°C. Upper panels show the residuals of fitting to a single exponential function (line in the lower panel). Residuals are shown as the percentages against overall change of the ellipticity. (B) An Arrhenius plot for the unfolding rate of OmpA at $X_{OG}=0$. The line is the best-fit straight line determined by the least-square procedure.

4. Discussion

In the present study, we demonstrated the multistep refolding process of OmpA in the mixed surfactant system of SDS and OG using three spectroscop-

ic probes. OmpA consists of a transmembrane N-terminal domain and a periplasmic C-terminal domain. Therefore, these two domains may fold with different kinetic phases, and such differences could be observed by far- and near-UV CD spectroscopies. However, the kinetic phases obtained from near-UV CD measurements were identical to those obtained from far-UV CD measurements (Fig. 5). The C-terminal domain of the protein is unknown but predicted to be flexible [17,18]. In addition, aromatic residues often affect the far-UV CD spectrum [23]. Therefore, the conformational change of the C-terminal domain may contribute little to the changes in the far-UV CD spectrum. Hence, our results do not exclude the possibility that folding of the N-terminal and C-terminal domains has distinct kinetics. Note that the data obtained through this study do not refer the folding and unfolding behavior of the C-terminal domain directly.

We found that the refolding rates of h-OmpA depend logarithmically on X_{OG} (Fig. 5). Assuming this correlation holds at lower X_{OG}, we estimated the refolding rate of the slowest phase at $X_{OG} = 0$ and 30°C to be 5.5×10^{-12} s^{-1}. We also estimated the unfolding rate of OmpA at $X_{OG} = 0$ and 30°C to be 9.6×10^{-9} s^{-1}. Thus, the unfolding rate of OmpA under these conditions was significantly larger than the refolding rate. The slow folding rate of a protein can be attributed to the height of the kinetic energy barrier between the unfolded state and the folded state [24]. At $X_{OG} = 0$ and 30°C, the energetic barrier, $\Delta G^{\ddagger}_{SDS}$, to unfolding and refolding of OmpA is calculated to be 28.9 kcal mol^{-1} and 33.3 kcal mol^{-1}, respectively, using Eyring's equation [25]:

$$\Delta G^{\ddagger}_{SDS} = RT \ln(k_B T / h k_{SDS}) \quad (2)$$

where k_B is Boltzmann's constant, h is Planck's constant and k_{SDS} is the rate constant in SDS solution. Thus, the folded form of OmpA is less stable than the unfolded form by 4.4 kcal mol^{-1}. Although this estimation through large extrapolations certainly contains large errors, it is consistent with the fact that OmpA in SDS solution maintains its folded structure at room temperature and the heat-modified form once obtained by heating remains unfolded by lowering the temperature.

OmpC [26] and OmpF [27] porins of *E. coli* are also known to maintain their folded structure in the oligomeric states in the presence of SDS. However, not all membrane proteins maintain their folded structure in the presence of SDS. For instance, bacterial opsins and diacylglycerol kinase readily denature in SDS solution [28,7], suggesting that the metastability of OmpA is not a common feature of membrane proteins. It should be noted that the metastable feature of OmpA in SDS solution does not necessarily imply the same feature of the protein in biomembranes. However, it is possible that proteins that reside on the bacterial outer membrane where they may be exposed to a severe environment acquire a unique mechanism to gain conformational stability, like an extracellular protease, α-lytic protease, retains a metastable form as its native form [29,30].

Our kinetic study using the mixed surfactant system revealed the metastable nature of the SDS-solubilized OmpA. Previously, Lau and Bowie provided an assessment of the thermodynamic stability for diacylglycerol kinase using a mixture of SDS and decyl maltoside [7]. However, the number of stability assessments obtained through such surfactant mixed systems is very small. Further studies of other membrane proteins with similar procedures would contribute to further understanding of the folding mechanism of membrane proteins.

Acknowledgements

We are grateful to Dr. Taiji Nakae for kindly providing the mutant strain of *E. coli*, TNE001. We thank Drs. Yuji Goto, Shohei Koide and Mark Dumont, and Franz Gruswitz for critical reading of the manuscript and fruitful discussion. This work is partially supported by Scientific Research Funds (grant Nos. 06808065 and 08272217) from the Ministry of Education, Science and Culture of Japan.

References

[1] K.S. Huang, H. Bayley, M.J. Liao, E. London, H.G. Khorana, Refolding of an integral membrane protein. Denaturation, renaturation, and reconstitution of intact bacteriorhodopsin and two proteolytic fragments, J. Biol. Chem. 256 (1981) 3802–3809.

[2] J.L. Popot, D.M. Engelman, O. Gurel, G. Zaccai, Tertiary structure of bacteriorhodopsin. Positions and orientations of helices A and B in the structural map determined by neutron diffraction, J. Mol. Biol. 210 (1987) 829–847.
[3] P.J. Booth, S.L. Flitsch, L.J. Stern, D.A. Greenhalgh, P.S. Kim, H.G. Khorana, Intermediates in the folding of the membrane protein bacteriorhodopsin, Nat. Struct. Biol. 2 (1995) 139–143.
[4] P.J. Booth, A. Farooq, S.L. Flitsch, Retinal binding during folding and assembly of the membrane protein bacteriorhodopsin, Biochemistry 35 (1996) 5902–5909.
[5] J.F. Hunt, T.N. Earnest, O. Bousche, K. Kalghatgi, K. Reilly, C. Horvath, K.J. Rothschild, D.M. Engelman, A biophysical study of integral membrane protein folding, Biochemistry 36 (1997) 15156–15176.
[6] P.J. Booth, H. Paulsen, Assembly of light-harvesting chlorophyll α/β complex in vitro. Time-resolved fluorescence measurements, Biochemistry 35 (1996) 5103–5108.
[7] F.W. Lau, J.U. Bowie, A method for assessing the stability of a membrane protein, Biochemistry 36 (1997) 5884–5892.
[8] J.L. Eisele, J.P. Rosenbusch, In vitro folding and oligomerization of a membrane protein. Transition of bacterial porin from random coil to native conformation, J. Biol. Chem. 265 (1990) 10217–10220.
[9] T. Surrey, A. Schmid, F. Jähnig, Folding and membrane insertion of the trimeric β-barrel protein OmpF, Biochemistry 35 (1996) 2283–2288.
[10] T. Surrey, F. Jähnig, Refolding and oriented insertion of a membrane protein into a lipid bilayer, Proc. Natl. Acad. Sci. USA 89 (1992) 7457–7461.
[11] T. Surrey, F. Jähnig, Kinetics of folding and membrane insertion of a β-barrel membrane protein, J. Biol. Chem. 270 (1995) 28199–28203.
[12] J.H. Kleinschmidt, L.K. Tamm, Folding intermediates of a beta-barrel membrane protein. Kinetic evidence for a multistep membrane insertion mechanism, Biochemistry 35 (1996) 12993–13000.
[13] J.H. Kleinschmidt, T. den Blaauwen, A.J.M. Driessen, L.K. Tamm, Outer membrane protein A of *Escherichia coli* inserts and folds into lipid bilayers by a concerted mechanism, Biochemistry 38 (1999) 4996–5005.
[14] J.H. Kleinschmidt, L.K. Tamm, Time-resolved distance determination by tryptophan quenching: probing intermediates in membrane protein folding, Biochemistry 38 (1999) 5006–5016.
[15] J.H. Kleinschmidt, M.C. Wiener, L.K. Tamm, Outer membrane protein A of *E. coli* folds into detergent micelles, but not in the presence of monomeric detergent, Protein Sci. 8 (1999) 2065–2071.
[16] S. Ohnishi, K. Kameyama, T. Takagi, Characterization of a heat modifiable protein, *Escherichia coli* outer membrane protein OmpA in binary mixed surfactant system of sodium dodecyl sulfate and octylglucoside, Biochim. Biophys. Acta 1375 (1998) 101–109.
[17] R. Morona, M. Klose, U. Henning, *Escherichia coli* K-12 outer membrane protein (OmpA) as a bacteriophage receptor: analysis of mutant genes expressing altered proteins, J. Bacteriol. 159 (1984) 570–578.
[18] H. Vogel, F. Jähnig, Models for the structure of outer-membrane proteins of *Escherichia coli* derived from Raman spectroscopy and prediction methods, J. Mol. Biol. 190 (1986) 191–199.
[19] A. Pautsch, G.E. Schulz, Structure of the outer membrane protein A transmembrane domain, Nat. Struct. Biol. 5 (1998) 1013–1017.
[20] A. Pautsch, G.E. Schulz, High-resolution structure of OmpA membrane domain, J. Mol. Biol. 298, 273–282.
[21] K. Nakamura, S. Mizushima, Effects of heating in dodecyl sulfate solution on the conformation and electrophoretic mobility of isolated major outer membrane proteins from *Escherichia coli* K-12, J. Biochem. 80 (1976) 1411–1422.
[22] K. Dornmair, H. Kiefer, F. Jähnig, Refolding of an integral membrane protein. OmpA of *Escherichia coli*, J. Biol. Chem. 265 (1990) 18907–18911.
[23] M.C. Manning, R.W. Woody, Theoretical study of the contribution of aromatic side chains to the circular dichroism of basic bovine pancreatic trypsin inhibitor, Biochemistry 28 (1989) 8609–8613.
[24] T.E. Creighton, The protein folding problem, in: R.H. Pain (Ed.), Mechanisms of Protein Folding, IRL Press at Oxford University Press, Oxford, 1994, pp. 1–25.
[25] A.A. Forst, R.G. Pearson, Transition-state theory; comparison of collision and transition state theories, in: Kinetics and Mechanism, 2nd edn., John Wiley and Sons, New York, 1961, pp. 93–99.
[26] K. Kameyama, T. Nakae, T. Takagi, Estimation of molecular weights of membrane proteins in the presence of SDS by low-angle laser light scattering combined with high-performance porous silica gel chromatography. Conformation of the trimer structure of porin of the *E. coli* outer membrane, Biochim. Biophys. Acta 706 (1982) 19–26.
[27] W.J. Rocque, E.J. McGroarty, Isolation and preliminary characterization of wild-type OmpC porin dimers from *Escherichia coli* K-12, Biochemistry 28 (1989) 3738–3743.
[28] Y. Sugiyama, Y. Mukohata, Dual roles of DMPC and CHAPS in the refolding of bacterial opsins in vitro, J. Biochem. 119 (1996) 1143–1149.
[29] J.L. Sohl, S.S. Jaswal, D.A. Agard, Unfolded conformations of alpha-lytic protease are more stable than its native state, Nature 395 (1998) 817–819.
[30] N.K. Sauter, T. Mau, S.D. Rader, D.A. Agard, Structure of alpha-lytic protease complexed with its pro region, Nat. Struct. Biol. 5 (1998) 945–950.
[31] P. Kraulis, MOLSCRIPT: a program to produce both detailed and schematic plots of protein structures, J. Appl. Crystallogr. 24 (1991) 946–950.